Defect-induced heterogeneous transformations and thermal growth in athermal martensite

Wenwu Cao and James A. Krumhansl
Laboratory of Atomic and Solid State Physics, Cornell University, Ithaca, New York 14853

Robert J. Gooding
Department of Physics, Queen's University, Kingston, Ontario, Canada
(Received 20 December 1989)

A continuum model is proposed to explain defect-mediated heterogeneous martensitic transformations. As an example, the square-rectangular proper ferroelastic phase transition is considered. The role of a defect is considered to provide an inhomogeneous stress field acting on the pure system. This stress field modifies the free-energy density and has the strongest effect around (at) the defect. Certain external stresses of the correct symmetry can increase the transformation temperature, and the portion of the system around the defect, and only this portion, will therefore have a higher transition temperature. Thus, these regions can be thermally triggered first to become nuclei of martensite upon cooling. The temperature dependence of the equilibrium size of martensite in the matrix of the high-temperature phase is modeled and calculated for a coherent interface under free-boundary conditions, in which a simple functional form is assumed to simulate the stress field produced by a slab inclusion and/or defect. The results qualitatively agree with experimental observations.

I. INTRODUCTION

A significant class of structural transformations is referred to as martensitic.[1] They are lattice displacive at the unit-cell level, but are distinguished from other displacive transformations by their development of (mesoscopic) structure at the micron level, such as twin bands in the product phase. Of particular interest is that subclass in which the product is "coherent" with the parent; the structure is reversible and there can be "shape memory."

The mesoscopic structure develops because martensitic transformations are discontinuous in the lattice parameters, so that as the product phase grows the stress at the parent-product interface can be relieved by twinning, thus developing the banded pattern. Before this pattern is finally reached, there is the question of how the transformation is initiated and proceeds—referred to as nucleation and growth. These two processes involve both time t and temperature T.

The classical nucleation theory deals with the evolution of new phases with respect to time. It was developed for the problem of liquid condensation from vapor phase,[2–7] where the complete phase transition can occur at a critical temperature. The heterogeneity of the transformation is the distribution of time delays of the transition process in different portions of the system. Once a critical temperature is reached, so that the nucleation starts, the entire system will eventually evolve to the low-temperature phase. There is no need for further adjustment of system temperature. The nucleation rate with time can be calculated based on the theory of metastable states.[6,8–10]

For a heterogeneous martensitic transformation, however, the nucleation and growth are not as simple, and it is found that the macroscopic development of the low-temperature phase involves both time and temperature. Experimentally, there are found to be two distinct classes of martensitic transformation: *athermal* and *isothermal*.[11] In the former class, as the temperature is lowered, at some start temperature isolated small regions of the martensitic product begin to appear in the parent phase. The transformation at any temperature appears to be *instantaneous* on practical time scales, and the amount of transformed material depends only on temperature, i.e., increasing with each step of lowering temperature. In the development of athermal martensite activation kinetics are secondary. The transition process will not be completed until system temperature is lowered further to M_F—a martensite finish temperature.

In the case of isothermal martensitic transition the situation is different. Martensite may start locally at a certain temperature, and then the size of martensitic regions increases continuously with time. There is no clear definition of martensite finish temperature, which depend only on how long one can wait. Theoretically speaking, the isothermal martensitic transition process could go to completion at one temperature; thus, further lowering of temperature can only augment the growth process. In any case, for isothermal martensite, transition kinetics is the central issue; the aging or ripening process is determined thereby. Considering the distinct properties of these two classes of martensite, it is apparent that the simple conceptual model of classical nucleation theory is not adequate to deal with all martensitic transformations. It may provide some framework for the isothermal-type transition, but for the athermal-type transition a new approach must be developed in order to address the thermal evolution. For heterogeneous athermal martensitic transitions, the initial martensitic regions appear at the mi-

croscopic scale (usually around defects[12–14]) and the kinetic processes are completed so fast that the low-temperature phase seems to be "thermally nucleated." The same is also true for the growth process: The development of martensite is represented by an equilibrium configuration that minimizes the total free energy of the system. An equilibrium size of the martensite is associated with each temperature,[15] and as temperature is lowered this size increases, which can be described as "thermal growth process." In general, martensite appears in isolated regions by the defects[12–14] and the eventual complete transformation involves overlap and interaction of the product domains developed from these regions.

Because of both experimental and theoretical developments over the past few years, we have chosen to examine a theoretical model of nucleation and growth at a defect, in the sense that it applies to athermal martensite. There is well documented experimental data now showing the appearance and disappearance of a martensitic phase at a defect, with cycling of temperature down and up.[12–15] At the same time nonlinear, nonlocal elasticity theories[16,17] have been developed over the past few years that we show can provide an effective basis for describing the local transformation to product due to the defect imposed stresses, as well as the thermal dependence of the transformed region.

In this paper, we apply a Ginzburg-Landau-type phenomenological continuum theory to the square-rectangular proper ferroelastic heterogeneous transition in 2D. To proceed we make two assumptions based on experimental facts. (i) It is the stress field produced by the defect but not the defect ("core") itself which is responsible for the heterogeneous nucleation. (ii) The interface of high- and low-temperature phases is coherent. Assumption (i) is based on the fact that *a priori* no particular defects are more favored than others to be nucleation centers. Experiments show these nucleation centers could be almost any kind of defects and are generally sample dependent. Assumption (ii) is to ensure the applicability of elastic continuum theory in dealing with the thermal growth process. It implies that the kinetic nucleation process of initial formation of the local micro- and/or mesoscopic martensite is coherent. In principle, the parent-product interface could also be semicoherent or incoherent; then the current theory has to be augmented in order to describe those systems.

The paper is arranged as follows: In Sec. II we introduce the theoretical model; Sec. III shows the effect of homogeneous stress on the transition temperature, and the local formation of martensite around the defect is discussed in Sec. IV. Then, the thermal growth of such localized regions of martensite in the austenite matrix is calculated in Sec. V. Lastly, Sec. VI contains our summary and conclusions.

II. THEORETICAL MODEL

The 2D model for the 4mm-2mm proper ferroelastic phase transition, without external stresses, was developed by Jacobs,[16] and Barsch and Krumhansl,[17] to study the interface boundaries between the energetically degenerate variants. The appropriate symmetry coordinates were defined to be

$$e_1=(\eta_{11}+\eta_{22})/\sqrt{2}\ , \tag{1}$$

$$e_2=(\eta_{11}-\eta_{22})/\sqrt{2}\ , \tag{2}$$

$$e_3=\eta_{12}\ . \tag{3}$$

Here $\eta_{ij}=\frac{1}{2}(u_{i,j}+u_{j,i}+u_{i,j}u_{j,i})$ are the components of the elastic strain tensor in Voigt notation, and u_i is the displacement field; e_1 is a dilational strain which does not change the symmetry of the system, and e_3 represents a shear strain which is not essential in the square-rectangular transformation. Only e_2, the deviatoric strain, is important for this case. Bearing this in mind, we can now write the total free energy for the system in the following form:

$$F=\int\int\int f(u_{i,j},u_{i,jk},\sigma_{ij})dV\quad (i,j,k=1,2)\ , \tag{4}$$

where σ_{ij} are the applied external stress components, and the indices after comma represent partial differentiations with respect to the corresponding space variables. Further,

$$f(u_{i,j},u_{i,jk},\sigma_{ij})=f_0+f_g \tag{5}$$

is the energy density composed of (i) f_0, the local strain energy density under external stress and which can be written, in terms of the symmetry coordinates defined in Eqs. (1)–(3), as

$$f_0=\frac{A_1}{2}e_1^2+\frac{A_2}{2}e_2^2+\frac{A_3}{2}e_3^2+Ge_1e_2^2+\frac{B_2}{4}e_2^4+\frac{C_2}{6}e_2^6-\sum_{\alpha=1}^{3}\sigma_\alpha e_\alpha\ , \tag{6}$$

and (ii) f_g, which represents the strain gradient energy and is given in terms of the symmetry coordinates as[17]

$$\begin{aligned}f_g=&\tfrac{1}{2}d_1(e_{1,1}^2+e_{1,2}^2)+\tfrac{1}{2}d_2(e_{2,1}^2+e_{2,2}^2)\\&+\tfrac{1}{2}d_3(e_{3,1}^2+e_{3,2}^2)+d_4(e_{1,1}e_{2,1}-e_{2,1}e_{2,2})\\&+d_5(e_{1,1}e_{3,2}+e_{1,2}e_{3,1})\\&+d_6(e_{2,1}e_{3,2}-e_{2,2}e_{3,1})\ .\end{aligned} \tag{7}$$

Here, all the coefficients in Eqs. (5) and (6) are assumed to be temperature independent except A_2.

The Lagrange density is

$$L(\dot{u}_i,u_{i,j},u_{i,kl},\sigma_{ij})=\tfrac{1}{2}\rho_0\dot{u}_i\dot{u}_i-f(u_{i,j},u_{i,jk},\sigma_{ij})\ , \tag{8}$$

where ρ_0 is the mass density. The equation of motion can be written as[16,17]

$$\rho\ddot{u}_i=\partial_j\frac{\partial f}{\partial u_{i,j}}-\partial_j\partial_k\frac{\partial f}{\partial u_{i,jk}},\quad (i,j,k=1,2)\ . \tag{9}$$

III. EFFECT OF HOMOGENEOUS STRESS

Before we solve the full equation of motion, viz. Eq. (9), let us look at some special cases. The simplest case would be when the system is homogeneous, i.e.,

$$\sigma_\alpha = \text{const} , \tag{10}$$

$$f_g = 0 . \tag{11}$$

The equilibrium conditions $\partial f_0/\partial e_\alpha = 0$, $\alpha = 1,3$ lead from Eq. (6) to

$$e_1 = \frac{\sigma_1 - G e_2^2}{A_1} , \tag{12a}$$

$$e_3 = \frac{\sigma_3}{A_3} . \tag{12b}$$

Substituting (12a) and (12b) into (6) gives us an effective elastic ϕ^6 model in terms of e_2

$$f_0' = f_0 + \tfrac{1}{2}\left[\frac{\sigma_1^2}{A_1} + \frac{\sigma_3^2}{A_3}\right] = \frac{A'}{2}e_2^2 + \frac{B_2'}{4}e_2^4 + \frac{C_2}{6}e_2^6 - \sigma_2 e_2 , \tag{13}$$

where

$$A_2' = A_2 + \frac{2G\sigma_1}{A_1} , \tag{14a}$$

$$B_2' = B_2 - \frac{2G^2}{A_1} . \tag{14b}$$

Since $A_1 > 0$ and $B_2 < 0$ for a first-order transition, B_2' is also negative.

When $\sigma_\alpha = 0$, $A_2' = A_2$ and we have the following solutions for the deviatoric strain e_2 from $\partial f'/\partial e_2 = 0$.

(i) $A_2 > B_2'^2/4C_2$: $e_2 = 0$, only the square phase is stable.

(ii) $0 < A_2 < B_2'^2/4C_2$: $e_2 = 0$, the square phase is locally stable; $e_2 = \pm e_2^r$, the rectangular phase is also locally stable, where

$$e_2^r = \left[\frac{-B_2' + (B_2'^2 - 4A_2'C_2)^{1/2}}{2C_2}\right]^{1/2}$$

(iii) $A_2 < 0$: $e_2 = \pm e_2^r$, only the rectangular phase is stable.

There is only one thermodynamically stable state at any given temperature, and therefore either the square or rectangular phase is metastable in region (ii). Theoretically speaking, a first-order phase transition can happen when $f'_{\text{square}} = f'_{\text{rectangular}}$. The strain e_2 and the transformation temperature are then determined by

$$e_2^2 = e_0^2 = -\frac{3B_2'}{4C_2} , \tag{15}$$

and

$$A_2 = \frac{3B_2'^2}{16C_2} . \tag{16}$$

Near the transition temperature, A_2 is generally written in the form

$$A_2 = \beta(T - T_c) ,$$

where β is positive and independent of temperature. The first-order transition temperature T_1 is then given by

$$T_1 = T_c + \frac{3B_2'^2}{16C_2} . \tag{17}$$

In order to study the case of constant $\sigma_\alpha \neq 0$, we rescale the strain and free-energy density as follows:

$$e_2 = e_0 \epsilon , \tag{18}$$

$$f_{\text{eff}} = f_0' \Big/ \left[-\frac{9B_2'}{64C_2^2}\right] = \tfrac{1}{2}\tau\epsilon^2 - \epsilon^4 + \tfrac{1}{2}\epsilon^6 - \sigma\epsilon . \tag{19}$$

Here

$$\tau = \frac{T - T_c}{T_1 - T_c} , \tag{20}$$

and

$$\sigma = \frac{16}{3}\frac{C_2}{B_2'}\left[\frac{4C_2}{-3B_2'}\right]^{1/2}\sigma_2 \tag{21}$$

are the effective temperature and stress, respectively. The equilibrium condition becomes

$$\tau\epsilon - 4\epsilon^3 + 3\epsilon^5 = \sigma . \tag{22}$$

The three temperature regions discussed above are shifted by the applied stress field. However, using the same framework one can derive the first-order transition temperature τ_1 according to

$$f_{\text{eff}}(\epsilon^s, \tau_1) = f_{\text{eff}}(\epsilon^r, \tau_1) , \tag{23}$$

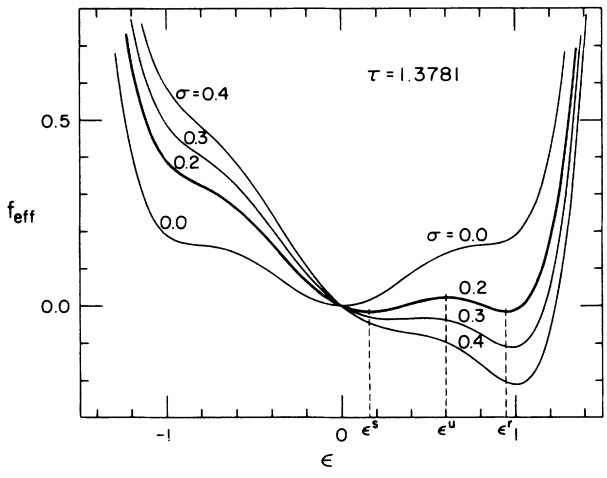

FIG. 1. Plot of the effective free-energy density under different homogeneous external stress σ for a given temperature $\tau = 1.3781$, which is the transition temperature for $\sigma = 0.2$. Here ϵ^s and ϵ^r represent the strain values for the distorted high-temperature and low-temperature phases, respectively.

where ϵ^s and ϵ^r are the corresponding strain values for the distorted square and rectangular phases, respectively, which are determined from Eq. (22).

Figure 1 shows the effective free energy density for $\sigma=0.2$ at $\tau_1=1.3781$, and for comparison, $\sigma=0$, 0.3, and 0.4 at the same temperature. It is clear that the external stress fields pushes the transformation to a higher temperature ($\tau_1=1$ for $\sigma=0$) in this model. A quantitative calculation of τ_1 versus σ is shown in Fig. 2, where region I is the distorted square phase and region II is the distorted rectangular phase, respectively. Two points need to be noted. The first is that there is a limiting stress of $\sigma=\sigma_c$. For $\sigma<\sigma_c$ the transition from region I to region II is first order; as σ increases, τ_1 increases, and at the same time the discontinuity of the order parameter at the transition becomes smaller. When $\sigma\geq\sigma_c$ the first-order transition will be smeared out and there will be no well defined τ_1. This is easy to understand from Eqs. (22) and (23); at $\sigma=\sigma_c$, the three roots become degenerate, i.e.,

$$\epsilon^s=\epsilon^u=\epsilon^r . \tag{24}$$

Here ϵ^u represents the strain value of energy maximum (see Fig. 1). For $\sigma>\sigma_c$, only one real root exists for Eq. (22) in any temperature region.

The second is that the effect of σ is symmetric in our 2D model, viz., if $\sigma<0$, we can use the negative solutions of Eq. (22) $-\epsilon^s, -\epsilon^u, -\epsilon^r$ representing the other variant of square-rectangular transformation. Therefore, only the magnitude $|\sigma|$ is important, and τ_1 will always be increased with applied stress. The influence of external stress on the transition temperature of a ferroelastic system in 3D has been studied by Pietrass[18] and Szabo.[19] The symmetry relation $\tau_1(\sigma)=\tau_1(-\sigma)$ does not hold in the cases they studied.

IV. LOCAL FORMATION OF MARTENSITE AROUND DEFECTS

When defects are present in the system, they produce inhomogeneous stress fields in the surrounding matrix. We assume that the matrix of the pure system can only feel the stress field produced by the defect, but does not depend sensitively on the details of the defect "core." Thus, we can remove these elastic singularities (core of defect) by effectively extending the stress field that the pure system feels back into the core region of defect in such a fashion that it maintains the stress field outside the core unchanged. In this way, we are allowed to utilize continuum theory for a system containing defects. This method is, in a sense, analogous to the continuum description of defects.[20] Since we are interested only in the system outside the core of defects, changes inside the core will not affect the underlying physics as long as the pure system feels the same environment. With this in mind, we treat the system with defects as a pure system under localized inhomogenous external stress. These inhomogeneous stress fields modify the free-energy density in space, and hence cause a spatial variation of transition temperature, according to the analysis in the last section.

To make the matter pedagogically clearer we look at the effect of the deviatoric stress $\sigma_2(\mathbf{r})$ only. For this case we can again use the effective energy density Eq. (19). Because σ now is inhomogeneous, the free-energy density will vary accordingly. To see this, one can refer to Fig. 1 in which curves associated with each σ represent free-energy densities at different locations in space.

Imagine cooling a system down from the high-temperature phase. At a given temperature $\tau>1$, while the majority of the system (far away from a defect) is still in the high-temperature phase (represented by the $\sigma=0$ curve in Fig. 1), some portion of the system close to the

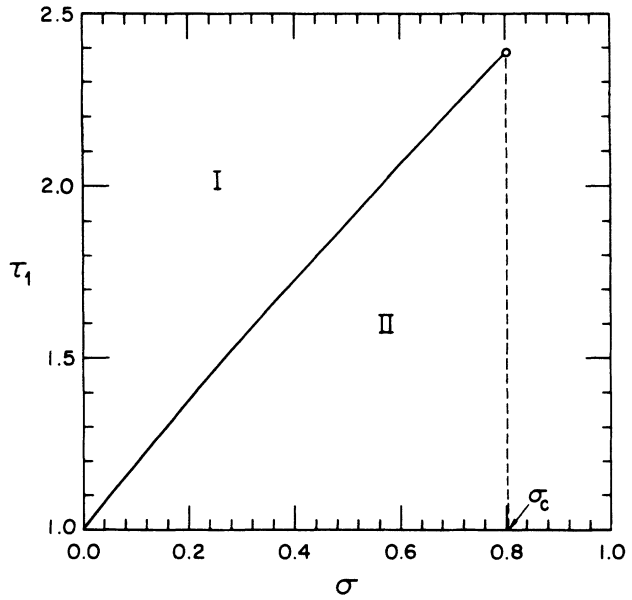

FIG. 2. Relation of the first-order transition temperature τ_1 and the applied homogeneous external stress σ, in dimensionless units.

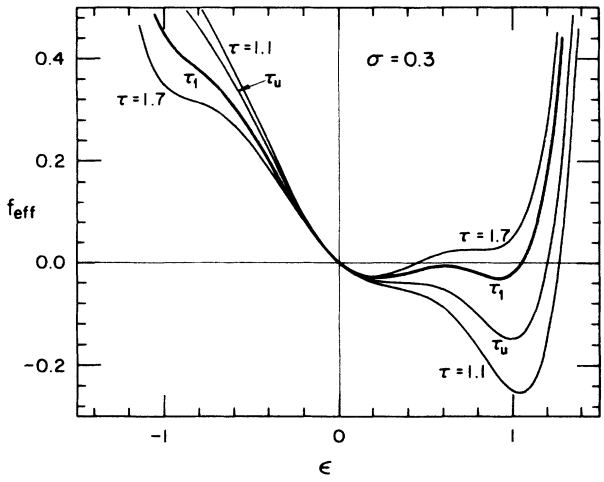

FIG. 3. Temperature dependence of the effective free-energy density under a given homogeneous external stress $\sigma=0.3$ in dimensionless units. $\tau_1=1.556$ is the temperature at which the free energies of high- and low-temperature phases are equal. $\tau_u=1.301$ is the temperature when the metastability vanishes for the high-temperature phase under the stress $\sigma=0.3$.

defect may be energetically favored to be in the low-temperature phase (represented by $\sigma > 0.2$ curves in Fig. 1). Therefore, at some critical temperature τ_s, some localized martensites will be thermally activated to form around defects in order to reduce the total energy of the system. For a given stress magnitude, two free-energy minima appear in some temperature range. A first-order phase transition can occur via thermal fluctuations at a temperature τ_s equal to or below τ_1, depending on the magnitude of fluctuations, as well as the transition barrier height. Without activation by thermal fluctuations the transition will not happen until the metastability vanishes, i.e., $\tau = \tau^u$ as shown in Fig. 3. In general, heterogeneous local transformations mediated by the stress field of defects are thermally activated and the so obtained isolated product phase regions could form coherently, semicoherently, or incoherently with the surrounding matrix, which would be determined by the initial nucleation mechanism. Here, these isolated product phase regions are very small when formed at their local critical temperature, and therefore the time evolution is not a crucial issue; so we will only focus on the thermal process in what follows.

V. THERMAL GROWTH OF MARTENSITE WITH A COHERENT INTERFACE

When the temperature coming from above reaches τ_s, the local transition temperature, some isolated coherent product phase of a microscopic size may form through fluctuation-mediated local transition. If temperature is cooled further, these product regions will grow. The equilibrium size at each temperature is determined by the minimization of total energy of the system (including the defect region).

As we have already discussed, the inhomogeneous stress field produced by defects causes the *local* transformation temperature to vary in space. If the system temperature is changed slowly we would expect a steady equilibrium growth pattern of the low-temperature phase in the high-temperature matrix. In this section we will illustrate the development of martensite around a defect by using the simplest example; it can at least qualitatively explain the experimental results of Saburi and Nenno.[14] Here we will only look at the growth of the locally transformed product phase through a coherent interface; no new defects are created at the interface of high- and low-temperature phases during the whole process. It is assumed that the original stress field (determined by defect distributions) will not be altered by the appearance of the low-temperature phase.

Since the stress field is inhomogeneous, we have to solve Eq. (9) in order to obtain the equlibrium configurations of the system. For the static solutions, the left side of Eq. (9) is zero, and one is left to consider two coupled time-independent differential equations for the displacement field $\mathbf{u}(X, Y)$. A quasi-one-dimensional solution is possible when the stress field $\sigma_2(X, Y)$ varies only in the direction of the interface normal, which corresponds to the physical situation of a slab defect inclusion in the high-temperature matrix.

For the martensitic transformation of 4mm-2mm, the lattice motion is a pure $\langle 11 \rangle / \langle 1\bar{1} \rangle$ shear. There are two possible low-temperature variants which are energetically degenerate. With the application of $\sigma_2(X, Y)$ the degeneracy will be lifted and the rectangular axis will have a preferred orientation, for example, if

$$\sigma_2 = \sigma_2(\hat{\mathbf{n}} \cdot \mathbf{R}) > 0, \quad \text{with } \hat{\mathbf{n}} = \frac{1}{\sqrt{2}}(1,1) ; \tag{25}$$

the displacement field $\mathbf{u}$ will have the form

$$\mathbf{u} = \hat{\mathbf{m}} v(\hat{\mathbf{n}} \cdot \mathbf{R}), \quad \text{with } \hat{\mathbf{m}} = \frac{1}{\sqrt{2}}(1,\bar{1}) , \tag{26}$$

Here $\hat{\mathbf{n}}$ is the interface normal direction. For convenience we introduce a new space variable X' along $\hat{\mathbf{n}}$:

$$X' = \hat{\mathbf{n}} \cdot \mathbf{R} . \tag{27}$$

If the geometrical nonlinearity is ignored the strain components in the symmetry coordinate can be derived as[17]

$$e_1 = 0; \quad e_2 = \frac{1}{\sqrt{2}} \frac{d}{dX'} v; \quad e_3 = 0 . \tag{28}$$

Thus, only one independent equation is obtained from Eq. (9), viz.,

$$\frac{d}{dX'} \left[\frac{\partial f}{\partial e_2} - d_2 \frac{d^2 e_2}{dX'^2} \right] = 0 . \tag{29}$$

For a single inclusion, its effect diminishes far away from the defect, i.e., for $X' = \pm \infty$ the system will be homogeneous and in the high-temperature phase ($e_2 \equiv 0$ for $T > T_1$). Therefore, we can integrate Eq. (29) once to give an inhomogeneous second-order nonlinear differential equation for e_2:

$$d_2 \frac{d^2 e_2}{dX'^2} = A_2 e_2 + B_2 e_2^3 + C_2 e_2^5 - \sigma_2(X') . \tag{30}$$

Again, we can rescale Eq. (30) to dimensionless form by using the substitutions given by Eqs. (18), (20), and (21),

$$\frac{d^2 \epsilon}{d\xi^2} = \tau\epsilon - 4\epsilon^3 + 3\epsilon^5 - \sigma(\xi) , \tag{31}$$

where

$$\xi = \delta^{-1} X', \quad \delta^2 = \frac{16 C_2 d_2}{3 B_2^2} ; \tag{32}$$

δ has the dimension of length.

The functional form of σ will be determined by the nature of the defect involved. Considerable efforts have been made in the calculation of the defect generated stress fields based on linear elasticity theory.[21–25] These results showed $\sigma \propto 1/|r|^n$, $n = 1-3$, far away from the defects. However, it is not clear when close to a specific defect what functional form best represents the stress field it produces, especially for a nonlinear system. It may not be a simple function, and in general, may not be a continuous function of infinite order since even the linear elasticity result $1/r^n$ diverges at the origin. Thus, for

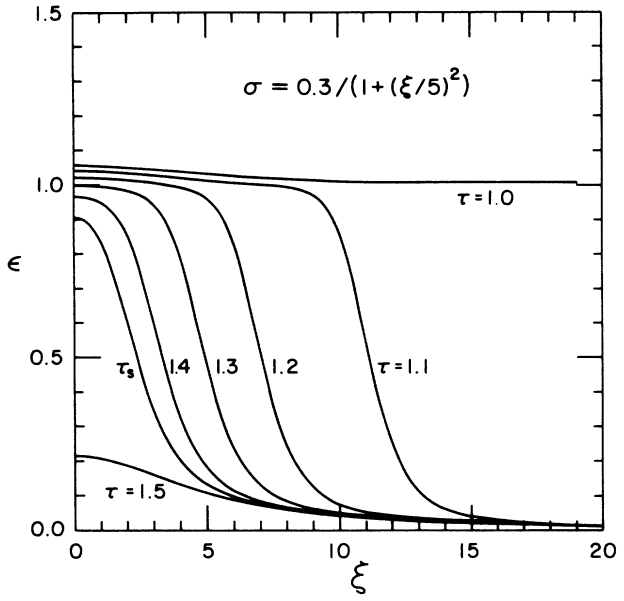

FIG. 4. Strain profiles for different temperatures under the stress field $\sigma=\sigma_0/[1+(\xi/\xi_0)^2]$ with $\sigma_0=0.3$, $\xi_0=5$. Here $\tau_s=1.4524$ is the local martensite formation temperature. For $\tau>\tau_s$ there is only pretransformed distortion of the high-temperature phase as shown by the curve $\tau=1.5$.

present exploratory purposes we choose a well-behaved model stress function which can be thought of to represent the stress field produced by a slab defect,

$$\sigma(\xi)=\frac{\sigma_0}{1+(\xi/\xi_0)^2}\ , \tag{33}$$

where σ_0 is the maximum stress magnitude, and $2\xi_0$ is the characteristic range of the model stress field. For any real situation the analysis can be carried out in the same fashion once the functional form of $\sigma(\xi)$ is given. We can then solve Eqs. (31) and (33) numerically. Noticing that ϵ is a symmetric function with respect to ξ for the given stress field, one can solve the problem in one half-space.

We now describe results for a choice of parameters $\sigma_0=0.3$, $\xi_0=5$, which correspond to, in the case of $In_{0.79}Tl_{0.21}$, $\sigma_{2\max}\sim 1.8$ bar and the characteristic range of the inclusion ~ 25 Å by using the data of Ref. 17. Figure 4 shows the rescaled strain ϵ profiles with respect to dimensionless variable ξ for a few temperatures ($\epsilon\sim 0$, distorted square phase; $\epsilon\sim 1$, distorted rectangular phase). One can see clearly the growth of martensite equilibrium size via a coherent interface when temperature is lowered. The displacement field **u** can be calculated easily from Eqs. (26) and (28), and the physical picture represented by the solutions is illustrated in Fig. 5. The width of the rectangular phase L is defined as the distance between the two points where the strain e_2 falls to half of its maximum value. The shaded area represents the part where the elastic discontinuity has been removed and replaced by crystal with no defects but with external stress present. One must remember that our "operation" is virtual, the stress field (defect) is always there. The form of the stress field being used will affect the thermal growth rate dL/dT (note T is temperature here). For the stress field given by Eq. (33), the martensite slowly grows with decreasing temperature at the beginning after it appears at $\tau=\tau_s$, but $|dL/dT|$ increases drastically as the bulk transformation temperature is approached.

Figure 6 displays the thermal growth of martensite under the stress field given in Eq. (33), where $l=L/\delta$ is the width of low-temperature phase in dimensionless units. At a certain temperature $\tau_s>1$, the martensite will form around defects with a finite size. Because the effect of a

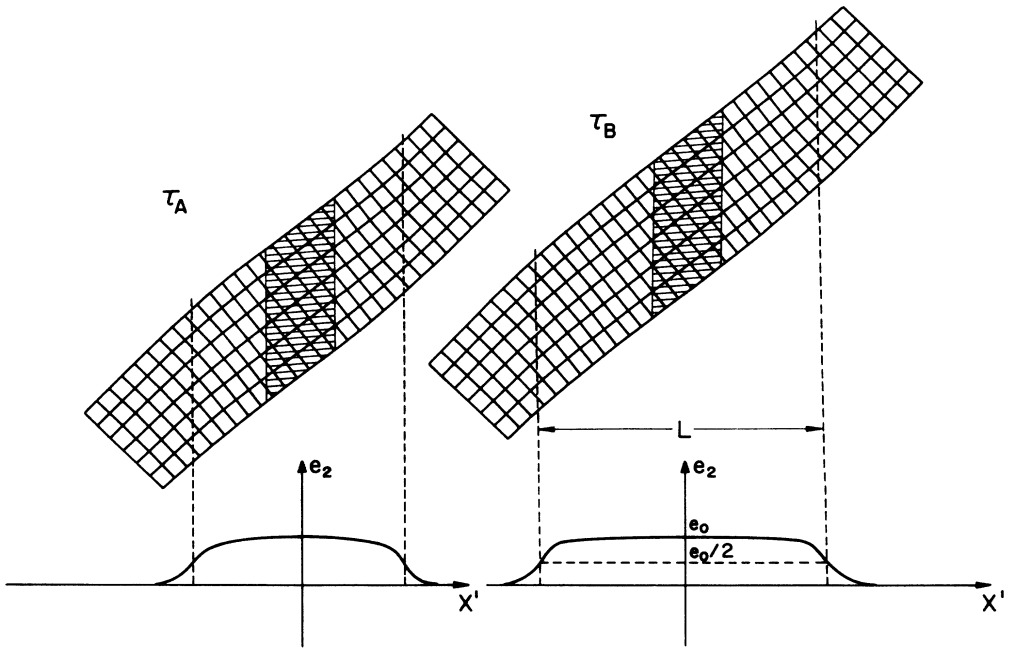

FIG. 5. Illustration of the growth pattern of martensite represented by the strain profile at two temperatures τ_A and τ_B, where $\tau_s>\tau_A>\tau_B>\tau_f$. The shaded area represents the slab inclusion of defects.

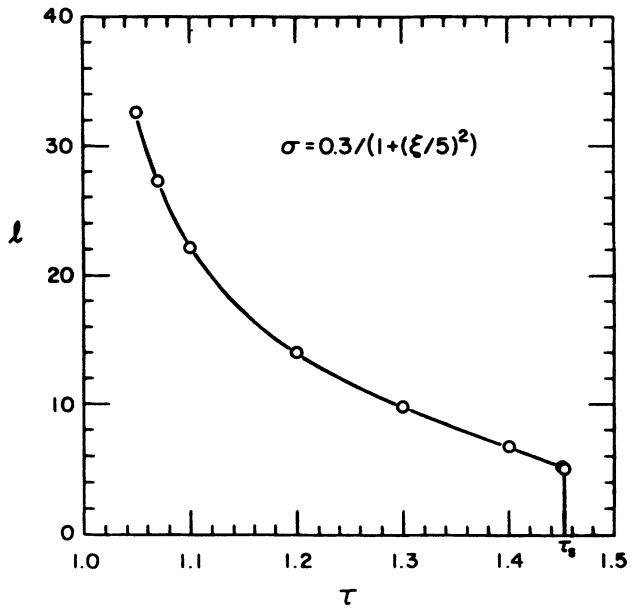

FIG. 6. Equilibrium size of martensite vs temperature in dimensionless units, for the given inhomogeneous external stress.

defect dies off quickly away from it, the amount of martensite increases with decreasing temperature relatively slowly at the beginning, or one might say that the transformed regions are quite "localized." There is a temperature range in which the growth of martensite can be clearly followed, as observed by Saburi and Nenno.[14] Unfortunately, the corresponding temperatures in their electron microscopy could not be determined, and that prevents the direct comparison of our theoretical results with their observations. Special attention needs to be given to the value τ_s, which is the highest possible temperature for local martensitic transition to occur in an inhomogeneous system. It is *neither* τ_1 *nor* τ_u, which were derived for the homogeneous system. The nonlocal (gradient) interaction for the inhomogeneous system provides a "dragging" force on each part of the system from its neighboring parts. This dragging makes the localized martensitic formation more difficult for the coherent nucleation to proceed, and therefore τ_s is lower than τ_1 (taking $\sigma_2|_{\max}$ as the homogeneous stress field), τ_s may also be lower than τ_u for large magnitude inhomogeneous stress, depending on how strong is the nonlocal coupling (gradient). The strain profile represents the minimum of total free energy; local martensite can be produced only when their production can reduce the total system free energy.

In this model we define the martensite finish temperature τ_f as the temperature at which l, the width of the martensite, goes to infinity. Far away from the defect, $\sigma_2 \sim 0$, the high-temperature phase could be still metastable for $\tau \lesssim 1$. However, with the help of the nonlocal dragging force, the already developed low-temperature phase portion will "pull" the bulk over the energy barrier to fall into the lower energy well through the coherent interface; thus it will reduce the total energy of the system. This dragging force may be much more important than that of the effect of thermal fluctuations to influence the bulk transformation. This effect is more pronounced if the model stress field has a longer range, and as a comparison we provide another set of numerical results where the stress $\sigma(\xi)$ is taken to have the following form:

$$\sigma(\xi)=\sigma_0 \exp\left[-\frac{\xi^2}{\xi_0^2}\right] . \tag{34}$$

Equation (34) has a shorter range compared to Eq. (33). The rescaled strain profiles calculated for several temperatures with $\sigma_0=0.3$ and $\xi_0=2$ are given in Fig. 7. It is found that the martensite develops later and more slowly with decreasing temperature compared to the situation of under the stress field given by Eq. (33).

For a system containing a single defect, the transformation finish temperature coincides with the bulk transition temperature, i.e., $\tau_f=1$ in the thermodynamical limit ($\tau_f \geq 1$ for a finite system with defect). With very large stress fields, our results also showed divergence of the interface solution of $\tau_f > 1$ even for an infinite system with single defect. In that case the divergence may not represent the completion of the transformation, but instead it may suggest a breakdown of the coherency between high- and low-temperature phases, i.e., the irreversible creation of interfacial defects. This agrees with the fact that our theory is meaningful only when the maximum external stress is within the elastic limit of the system (no plastic deformation). In real situations the system will have many defects present, and the system is also finite, so it is possible that the transformation finish temperature will be higher than for an ideal crystal. However, one must remember that the system becomes much more complicated since the induced stress can no longer be ignored. The effective stress $\sigma_2(\mathbf{r})$ will not only

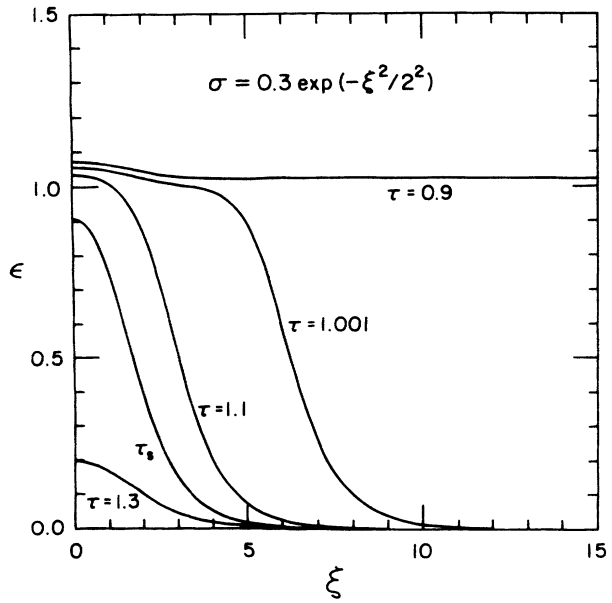

FIG. 7. Profiles of the rescaled deviatoric strain ϵ for different temperature with the assumed inhomogeneous applied stress field $\sigma=\sigma_0 \exp(-\xi^2/\xi_0^2)$, with $\sigma_0=0.3$, $\xi_0=2$. The local martensite start temperature is $\tau_s=1.2636$.

depend on position and direction but also on temperature. In principle the problem can still be solved self-consistently following the preceding procedure although that has not been done so far.

The results of this section are in interesting analogy with a situation in superconductivity. Twin boundaries have been observed to raise the superconducting transition temperature in some metals by as much as a factor of 2.[26] In fact, a static mechanism proposed was the local enhancement of T_c by the (defect) twin boundary,[27–29] which causes a proximity effect in the bulk. This was treated by a static heterogeneous Ginzburg-Landau model. The amount of transformed material depended on temperature above the bulk transition temperature.

VI. SUMMARY AND CONCLUSION

A continuum model has been constructed to describe the heterogeneous athermal martensitic transformation and the steady-state configuration of mixed high- and low-temperature phases for different temperatures in 2D. It is first proven that the transition temperature can be raised by the proper application of a homogeneous external stress field to the system. Therefore, an inhomogeneous stress field will cause a spatial variation of the transition temperature, if each small volume element is viewed as quasihomogeneous. The effects of a defect are considered primarily to create inhomogeneous stress fields which die off away from the defect. The elastic discontinuity at a defect core is removed by simulating the stress field in the system by a proper function $\sigma_2(\mathbf{r})$, which should coincide with the stress field produced by the defect outside the core region. The fact that heterogeneous martensite transformation nearly always starts from defects is easily explained by our model theory. The quantitative difficulty is the determination of the proper form of $\sigma_2(\mathbf{r})$ which would require some accurate elastic measurements. Once $\sigma_2(\mathbf{r})$ is known, the steady size of martensite can be calculated for any given temperature. We have demonstrated in this paper [for two choices of the function $\sigma_2(\mathbf{r})$] how a slab martensite grows with temperature for a coherent interface under free boundary conditions. Within the present model coherent growth and retraction are possible when the temperature is cycled. Our results can reasonably explain the experimental observations of Ref. 14 even with an assumed form of $\sigma_2(\mathbf{r})$.

The converse is also true, i.e., if the growth pattern around defects is known for any given temperature, we can also infer the proper form of $\sigma_2(\mathbf{r})$ close to a defect. Hopefully the sample temperature in an electron microscopy experiment will be measured in the near future, which will, together with our model, increase the level of understanding of the nucleation and growth process in martensitic transformations. In order to test our theory one can do the electron microscopy under an inhomogeneous stress field, and then watch the growth pattern with temperature as well as with the applied stress magnitude.

It must be pointed out that we have only considered the case for which the low-temperature phase forms into a single domain. In reality twins or twin bands may appear due to the induced elastic stress field even for a single defect, especially when the system has fixed boundary conditions. There is a finite coherency length at any temperature representing the maximum size of a single-domain martensite, which depends on the material properties, induced stress field, and the defect distribution.

There are some limitations for the present model, such as the truncation error in the free-energy expansion and the neglect of the geometrical nonlinearly in the calculation of the interface between the high- and low-temperature phases. Nevertheless, the approach provides a very simple conceptual way of dealing with the defect-mediated heterogeneous martensitic transformations in an athermal martensite, without having to know the microscopic details of the defect. Another novel feature in this paper is that we have derived interface strain solutions between energetically nondegenerate states which can exist only in the presence of inhomogeneous stress fields.

ACKNOWLEDGMENTS

We thank G. R. Barsch, B. Horovitz, and L. E. Tanner for useful discussions. We are also indebted to D. S. Liebermann for informative discussions of martensitic categories. This research was supported by the U.S. Department of Energy under Contract No. DE-FG02-88-ER45364, as well as by the Natural Sciences and Engineering Research Council of Canada.

[1] J. W. Christain, *The Theory of Transformations in Metals and Alloys*, 2nd ed. (Pergamon, Oxford, 1975).
[2] M. Volier and A. Weber, Z. Phys. Chem. **119**, 277 (1926).
[3] L. Farkas, Z. Phys. Chem. **125**, 236 (1927).
[4] M. Volmer, Z. Elektrochem. **26**, 555 (1929).
[5] R. Kaischew and I. N. Stranski, Z. Phys. Chem. B **26**, 317 (1934).
[6] R. Becker and W. Doering, Ann. Phys. (Leipzig) **24**, 719 (1935).
[7] J. Frenkel, J. Phys. (Paris) **1**, 315 (1939).
[8] J. S. Langer, Ann. Phys. (N.Y.) **54**, 258 (1969).
[9] J. S. Langer, Ann. Phys. (N.Y.) **65**, 53 (1971).
[10] J. S. Langer, Physica **73**, 61 (1974).
[11] K. C. Russel, Adv. Colloid Interface Sci. **13**, 205 (1980).
[12] P. L. Ferroglio and K. Mukherjee, Acta Metall. **22**, 835 (1974).
[13] J. W. Brooks, M. H. Loretto, and R. E. Smallman, Acta Metall. **27**, 1829 (1979).
[14] T. Saburi and S. Nenno, in *Proceedings of the International Conference on Martensitic Transformations (ICOMAT-86)*, edited by I. Tamura (The Japan Instutite of Metals, Sendai, 1987), p. 671.
[15] T. Saburi (private communication).
[16] A. E. Jacobs, Phys. Rev. B **31**, 5984 (1985).
[17] G. R. Barsch and J. A. Krumhansl, Metal. Trans. **19A**, 761

(1988).
[18]B. Pietrass, Phys. Status Solidi B **68**, 553 (1975).
[19]N. Szabo, J. Phys. C **8**, L397 (1975).
[20]C. Teodosiu, *Elastic Models of Crystal Defects* (Springer, Berlin, 1982).
[21]J. D. Eshelby, Proc. R. Soc. London, Ser. A **241**, 376 (1957).
[22]J. D. Eshelby, Proc. R. Soc. London, Ser. A **252**, 561 (1959).
[23]A. D. Brailsford, Phys. Rev. **142**, 383 (1966).
[24]L. J. Walpole, Proc. R. Soc. London, Ser. A **300**, 270 (1967).
[25]P. H. Dederichs and J. Pollmann, Z. Phys. **255**, 315 (1972).
[26]B. Horovitz, G. R. Barsch, and J. A. Krumhansl, Phys. Rev. B **36**, 8895 (1987).
[27]I. N. Khlyustikov and M. S. Khaikin, Pis'ma Zh. Eksp. Teor. Fiz. **38**, 191 (1983) [JETP Lett. **38**, 224 (1983)].
[28]I. N. Khlyustikov and S. I. Moskvin, Zh. Eksp. Teor. Fiz. **89**, 1846 (1985) [Sov. Phys. JETP **62**, 1065 (1986)].
[29]V. V. Averin, A. I. Buzdin, and L. N. Bulaevskii, Zh. Eksp. Teor. Fiz. **84**, 737 (1983) [Sov. Phys. JETP **57**, 426 (1983)].